41. INTERSTITIAL WATER CHEMISTRY, DEEP SEA DRILLING PROJECT, LEG 96[1]

B. J. Presley and Steven Stearns, Texas A&M University[2]

ABSTRACT

On Leg 96 of the Deep Sea Drilling Project (DSDP), holes were drilled in Orca and Pigmy basins on the northern Gulf of Mexico continental slope and on the Mississippi Fan. The holes on the fan encountered interbedded sand, silt, and mud deposited extremely rapidly, most during late Wisconsin glacial time. Pore-water chemistry in these holes is variable, but does not follow lithologic changes in any simple way. Both Ca and SO_4 are enriched in the pore water of many samples from the fan. Two sites drilled in the prominent central channel of the middle fan show rapid SO_4 reduction with depth, whereas two nearby sites in overbank deposits show no sulfate reduction for 300 m. Calcium concentration decreases as SO_4 is depleted and Li follows the same pattern. Strontium, which like Li, is enriched in samples enriched in Ca, does not decrease with SO_4 and Ca. Potassium in the pore water decreases with depth at almost all sites.

Sulfate reduction was active at the two basin sites and, as on the fan, this resulted in calcium carbonate precipitation and a lowering of pore water Ca, Mg, and Li. The Orca Basin site was drilled through a brine pool of 258‰ salinity. Pore-water salinity decreases smoothly with depth to 50 m and remains well above normal seawater values to the bottom of the hole at about 90 m. This suggests constant sedimentation under anoxic hypersaline conditions for at least the last 50,000 yr.

INTRODUCTION

On Leg 96 of the Deep Sea Drilling Project, samples were collected from nine sites on the Mississippi Fan and from two intraslope basins on the northwest Gulf of Mexico continental slope (Fig. 1). As is discussed in the introductory chapter (this volume), the Mississippi Fan is a 300,000-km^2 accumulation of terrigenous sediment which can be divided into upper, middle, and lower fan regions. Only the middle and lower fan, where water depths are typically 2500 to 3000 m, were sampled on Leg 96. Most drill sites penetrated only the youngest fan lobe of this thick sediment pile and recovered sediments of mostly Ericson Zone Y age (Ericson and Wollin, 1968; see site chapters, this volume). Sedimentation rates in the Mississippi Fan were extremely rapid during the late Wisconsin glacial time, averaging more than 11 m/1000 yr. in the middle fan region, and more than 5 m/1000 yr. on the lower fan (site chapters, this volume). Abundant sand was encountered at the fan drill sites even though the nearest source for it is hundreds of kilometers away. The channel of the youngest fan lobe was apparently an effective conduit for moving near-shore sediment into deep water during glacial periods. Relative amounts of sand, silt, and mud vary greatly from site to site and with depth at any given site depending on the morphologic location of each on the fan and the changes in depositional processes (see site chapters, this volume).

The two intraslope sites, Orca Basin (Site 618) and Pigmy Basin (Site 619), contain predominantly fine-grained hemipelagic and pelagic sediments with only localized coarser grained layers.
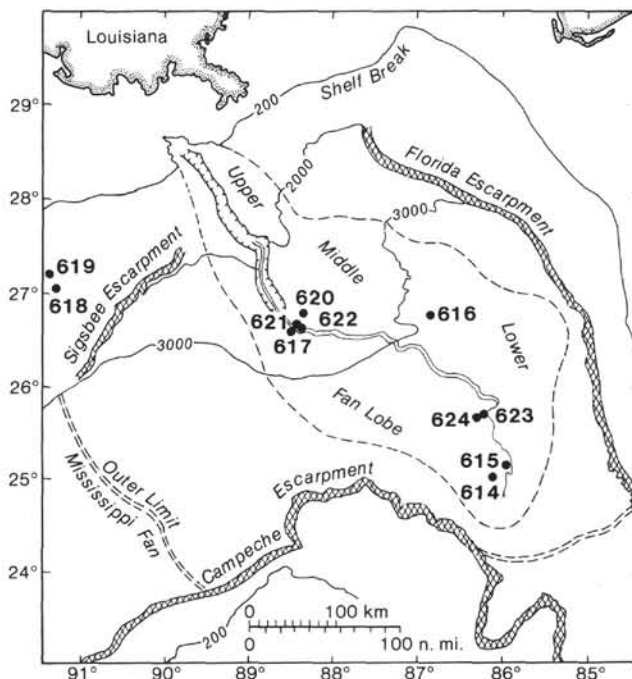

Figure 1. Site map showing locations drilled off Louisiana on Leg 96 of the Deep Sea Drilling Project.

The chemistry of Leg 96 pore waters varies considerably from site to site and with depth at single sites, but these variations do not seem to be related in any simple way to variations in grain size or sedimentation rate, factors shown to be important in other studies (Manheim and Sayles, 1974; Presley and Trefrey, 1980; Gieskes, 1983). Pore-water variations between closely adjacent sites (e.g., 617 and 621, Fig. 1) are especially surprising, and, as is discussed below, may be more closely related to physical oceanography than to mineralogy and sedimentology.

METHODS

Pore water was expressed from sediment on the ship by stainless steel squeezers essentially as described by Manheim and Waterman (1974). The water was then membrane filtered and analyzed on ship for pH, alkalinity, and other parameters as described by Ishizuka, Kawahata, et al. (this volume). The water samples that we analyzed on-shore were splits of the shipboard samples which were heat sealed into sections of polyethylene tubing (the standard DSDP storage technique) and hand-carried to Texas A&M after the cruise. The samples were stored frozen for about 2 months before analysis began. They were thawed and aliquots were removed for CO_2, SO_4, and other analyses by Kennicutt et al. (for results see Kennicutt et al., this volume). The samples were then refrozen for several weeks before our work began.

The samples were allowed to thaw in our laboratory and were transferred to plastic vials. We feel that this procedure altered several of the samples because they proved to be 10–15% lower in salinity than adjacent samples, but had normal ion to Cl ratios. Our explanation is that these samples were transferred before salts precipitated during freezing could redissolve. Shipboard salinity measurements and Ishizuka's laboratory data show normal salinities for the samples we found depleted. Luckily, only a few samples were affected and no overall trends in the data were obscured.

Aliquots were removed from the approximately 10 ml of water in the vials for the various determinations we made (Table 1). Methods were essentially those described by Presley (1971), therefore only about 3 ml total volume was used for the analytical work. Chloride was titrated with silver nitrate using 1 ml of sample and directly rationing the volume of silver nitrate used to that needed to titrate 1 ml of Copenhagen standard seawater. Major cations were determined by atomic adsorption after adding 0.1 ml of sample to 10 ml of $LaCl_3$ solution (Ca, K) and further diluting that 0.1 to 10 with distilled water (Na, Mg). Standard seawater carried through the same dilutions was used for calibration.

A 4 to 1 dilution was made with $LaCl_3$ solution and Sr, Mn, and Fe were determined on this by atomic absorption using spiked seawater as standards. Lithium was determined on the raw sample by atomic absorption using standard seawater spiked with additional Li for calibration. Silicon was determined colorimetrically by a slight modification of the Strickland and Parsons (1968) method. The sulfate values given in this chapter were provided by Dr. James Brooks and were obtained by a turbidimetric method (see Kennicutt et al., this volume).

Despite the availability of water, no replicate analyses were made. The data quality can be judged by cation–anion balance, which was within 5% for most of the samples and in no case was off by as much as 10%. A similar test is to compare the ion to chloride ratios of the Gulf of Mexico surface seawater samples collected with the pore waters to ratios for standard seawater. We analyzed eight of these samples at the same time and in exactly the same way as the pore waters were handled (one analysis only per sample). Despite the fact that some of these samples had been diluted by the freezing and transferring procedure described earlier, the ion to Cl ratios were all within a few percent of the expected value. The actual ratios for the surface seawater are given in Table 2.

Our data can also be compared to that of Ishizuka, Kawahata, et al. (this volume). At the time of this writing, we had converted a limited amount of the data to the same units so as to directly compare it, and the agreement for most elements seems good. We obtained much higher values of Li for some samples and, in general, our Cl values are higher and our Ca and Mg values are lower. The data, however, follow similar trends in both data sets.

RESULTS AND DISCUSSION

Sites 614, 615, and 623 (Lower Mississippi Fan)

These holes are relatively close together near the lower end of the fan channel. Hole 614 was only drilled to 150 m sub-bottom because of equipment problems in stiff clay and loose sand, whereas Hole 615 was the deepest hole drilled on Leg 96, penetrating over 500 m of material similar to that in Hole 614 (see site chapters, this volume). The pore-water trends are distinct but can only be compared in the upper section because of contrasting hole depths.

Calcium concentration is surprisingly high in Hole 614, with even the shallowest sample (3 m sub-bottom) being enriched by 25% over normal seawater. This enrichment occurs only below 30 m in Hole 615 and increases erratically to 240 m with some values more than 50% above seawater in that interval (Fig. 2). Hole 614 pore water has near-seawater sulfate values throughout its 150-m depth; this trend holds to about 300 m in Hole 615. Below 300 m in Hole 615, the sulfate concentration starts to decrease markedly, going to 0 at 448 m (Fig. 2). This presumably biological sulfate reduction must produce bicarbonate alkalinity as can be shown in the following simplified way:

$$2 \, CH_2O + SO_4^{2-} = H_2S + 2 \, HCO_3^- \qquad (1)$$

The equation shows that 2 moles of bicarbonate are produced for each mole of sulfate reduced, thus for complete reduction of 25 mmol of sulfate as happens below 300 m depth in Hole 615, 50 mmol of bicarbonate would be produced. The shipboard measured alkalinity increase, in contrast, was only about 2 mEq/L (Ishizuka, Kawahata, et al., this volume). The missing alkalinity (HCO_3^-) has been used in precipitating calcium carbonate and other solids, and this is shown by the decrease in calcium in the pore water (Fig. 2). Calcium decreases from about 30 to about 10 mEq/L over the interval of the sulfate reduction thus accounting for much, but not all, of the alkalinity loss.

Magnesium was also lost from the pore water as sulfate was reduced, thereby using up additional alkalinity. The magnesium trend at Hole 615 is, in fact, similar to that of calcium, in that it starts at near-seawater values, goes through a broad erratic maximum, and then declines in the sulfate-reduction interval downhole. Sulfate reappears in the bottom three samples of Hole 615. These samples are from carbonate-rich oozes deposited during Wisconsin interglacial times, unlike most of the hole which penetrated carbonate-poor mud and sand of glacial times. Diffusion through the pore water has, of course, altered concentration trends and may control them in these deep samples, which may be fed by a deeper source of SO_4 and Ca.

Strontium concentration increases with Ca but levels off at values about 50% above surface values except for the 300% enrichment in the first two samples taken from the carbonate ooze at the bottom of the hole. The increase most likely results from carbonate dissolution and recrystallization which must have been particularly intense in Cores 615-49 and 615-50. Strontium showed the same 50% increase in many other pore-water samples from the fan, but the 300% enrichment seen in Cores 615-49 and 615-50 was not seen elsewhere on Leg 96. Neither, however, were the interglacial oozes sampled elsewhere on the fan.

Lithium concentration trends at Site 615 are similar to those of Ca, Mg, and Sr with a maximum of about 2 times seawater at 200 m sub-bottom and decreases to near seawater values toward the top and bottom of the

Table 1. Element concentrations in pore-water samples, DSDP Leg 96.

Core-Section (interval in cm)	Sub-bottom depth (m)	Cl (g/kg)	SO$_4$ (g/kg)	Na (g/kg)	K (mg/kg)	Mg (mg/kg)	Ca (mg/kg)	Sr (mg/kg)	Li (μg/kg)	Fe (mg/kg)	Mn (mg/kg)	Si (mg/kg)
Hole 614[a]												
1-2, 140–150	2.95	19.5	2.73	10.6	360	1290	530	11.1	230	4.9	0.70	10.2
2-2, 140–150	12.35	19.6	2.68	10.6	238	1355	572	13.3	250	1.7	0.45	13.0
3-2, 140–150	21.65	19.4	2.73	10.8	238	1395	508	13.3	265	2.4	0.40	13.5
Hole 614A[b]												
2-2, 140–150	47.95	19.7	2.73	10.8	305	1335	481	12.9	215	0.4	0.45	14.0
5-1, 134–134	71.49	19.5	2.73	10.6	261	1395	466	13.2	230	<0.1	0.25	11.5
11-1, 140–150	128.45	19.9	2.58	10.2	368	1650	504	13.3	285	<0.1	0.45	11.5
Hole 615[c]												
1-1, 132–142	1.37	16.5	2.58	9.3	370	1060	356	7.3	145	<0.1	0.75	8.3
2-2, 140–150	5.55	19.6	2.20	10.6	315	1235	356	9.2	120	<0.1	0.35	11.1
3-2, 140–150	15.05	17.2	2.11	9.3	219	1140	385	10.5	120	<0.1	0.25	11.0
5-2, 140–150	32.55	19.3	2.28	10.2	265	1265	534	12.0	255	<0.1	0.40	9.5
6-2, 140–150	42.05	17.3	2.40	9.6	244	1170	458	12.3	230	<0.1	0.35	9.3
7-5, 140–150	55.85	19.5	2.58	10.6	318	1305	561	13.3	240	<0.1	0.45	5.7
8-1, 140–150	59.15	17.4	2.40	9.6	244	1225	542	12.4	255	<0.1	0.40	8.4
9-2, 140–150	70.26	19.5	2.50	10.6	305	1245	606	13.0	290	1.8	0.15	10.0
11-2, 132–142	89.07	19.7	2.32	10.7	263	2000	447	13.3	180	1.2	0.15	11.5
12-2, 140–150	99.13	19.1	2.58	10.7	326	1355	455	13.8	165	<0.1	0.25	9.3
19-1, 140–150	163.65	19.3	2.58	10.6	318	1395	527	12.7	325	<0.1	<0.05	8.0
22-5, 132–142	198.07	18.6	2.39	10.7	194	1475	671	13.9	420	0.3	0.20	12.3
23-1, 140–150	201.65	17.1	2.41	9.6	292	1315	527	13.0	370	0.2	0.10	8.0
27-1, 140–150	239.65	19.6	2.54	10.7	353	1325	587	13.3	345	<0.1	<0.05	9.0
33-1, 140–150	306.15	19.6	1.96	10.8	345	1210	504	13.0	275	0.2	0.10	10.4
34-2, 140–150	317.15	18.8	1.80	10.2	337	1160	496	13.2	285	<0.1	0.05	9.1
38-1, 140–150	353.65	19.4	0.91	10.8	303	1500	307	13.2	205	0.6	0.05	8.1
40-1, 132–142	372.57	19.4	0.47	10.3	263	1070	250	13.8	170	<0.1	0.10	10.1
47-1, 138–150	448.64	19.7	0.00	10.8	248	1040	159	18.2	145	<0.1	0.10	10.0
49-2, 138–150	478.64	19.7	0.02	10.8	389	935	201	35.5	265	<0.1	<0.05	15.0
50-2, 138–150	488.14	19.3	0.06	10.4	374	925	189	35.2	195	<0.1	<0.05	18.0
52-1, 132–144	505.58	17.7	0.89	10.1	263	915	235	13.5	165	<0.1	0.15	6.0
Hole 615A[d]												
1,CC	5.55	19.6	2.20	10.6	—	1245	235	10.3	125	1.1	0.30	9.5
12,CC	153.58	19.5	2.63	10.4	267	1345	496	12.6	400	<0.1	0.10	11.1
Hole 616[e]												
1-1, 140–150	1.45	17.0	3.01	9.3	311	1130	436	7.6	310	<0.1	0.15	10.8
2-3, 140–150	10.55	19.4	3.21	10.3	252	1455	587	11.0	680	1.7	0.20	12.5
3-3, 140–150	20.05	19.4	3.31	10.3	254	1475	600	11.0	775	0.8	0.15	12.3
4-1, 140–150	26.55	17.2	3.31	10.7	244	1640	538	11.2	745	<0.1	0.15	11.8
5-3, 140–150	39.05	19.6	3.64	10.7	246	1570	720	11.3	910	0.8	0.15	14.3
6-1, 140–150	45.65	19.1	3.64	10.3	263	1540	614	11.2	785	1.5	0.20	11.3
7-4, 138–150	59.74	19.3	3.26	10.4	246	1520	604	11.2	690	3.4	0.20	13.0
8-1, 138–150	64.84	19.4	3.26	10.5	301	1440	638	11.9	655	2.4	0.65	12.3
9-3, 138–150	77.44	19.1	3.43	10.2	242	1465	616	11.6	585	1.0	<0.05	11.3
10-2, 138–150	85.54	19.2	3.17	10.2	225	1455	665	11.6	565	1.1	0.20	12.3
11-2, 138–150	95.14	17.9	3.06	9.8	238	1335	638	11.6	485	0.3	0.15	9.0
16-2, 138–150	145.34	19.1	2.91	10.1	196	1435	668	12.4	375	<0.1	0.15	8.8
17-2, 138–150	154.94	19.5	2.46	—	313	—	507	13.2	265	3.6	0.25	13.5
18-1, 138–155	163.64	19.5	2.37	10.8	374	1245	424	12.7	225	<0.1	<0.05	7.0
21-3, 66–78	193.92	19.3	2.73	11.0	292	1335	616	13.1	290	<0.1	0.15	9.5
24-1, 138–150	249.14	19.1	2.73	10.4	330	1325	593	13.8	275	<0.1	0.55	11.7
28-1, 138–150	306.74	19.0	2.37	10.1	210	1445	556	13.1	495	<0.1	0.10	11.0
30-2, 138–150	327.24	19.1	2.50	9.8	189	1395	676	13.4	425	<0.1	0.30	11.
32-2, 138–150	346.04	18.8	2.11	9.7	185	1375	657	13.5	460	<0.1	0.35	10.4
33-1, 138–150	353.84	19.1	2.19	9.8	185	1445	683	14.4	475	0.8	0.45	13.5
34-2, 138–150	364.64	18.4	2.07	9.8	185	1455	571	13.2	455	0.5	0.15	9.3
Hole 616A[f]												
2-2, 138–150	106.54	18.8	3.22	10.4	206	1425	751	12.4	485	1.2	0.20	12.8
4-2, 138–150	125.74	19.3	3.31	10.8	221	1415	773	12.5	495	12.1	0.35	15.2
Hole 617[g]												
1-2, 140–150	2.95	18.4	2.71	10.3	326	1235	413	8.3	125	5.5	0.30	9.4
2-2, 140–150	10.95	19.2	2.71	10.4	236	1335	503	10.2	170	<0.1	0.35	13.3
3-2, 140–150	20.55	19.2	2.86	10.0	210	1435	627	10.8	425	0.6	0.15	12.5
4-2, 138–150	30.14	19.2	3.24	10.4	256	1435	618	10.8	430	0.9	0.25	11.6
5-3, 140–150	41.25	19.3	3.40	10.4	286	1335	703	11.6	425	<0.1	0.20	6.1

Table 1 (continued).

Core-Section (interval in cm)	Sub-bottom depth (m)	Cl (g/kg)	SO₄ (g/kg)	Na (g/kg)	K (mg/kg)	Mg (mg/kg)	Ca (mg/kg)	Sr (mg/kg)	Li (µg/kg)	Fe (mg/kg)	Mn (mg/kg)	Si (mg/kg)
Hole 617[g] (Cont.)												
6-3, 138–150	50.74	19.4	3.02	10.4	240	1395	722	12.2	440	<0.1	0.15	8.0
7-2, 138–150	58.74	19.3	3.19	10.4	257	1365	718	12.3	400	2.8	0.35	10.1
8-3, 138–150	69.74	16.2	3.34	9.0	202	1170	603	10.2	315	<0.1	0.15	8.0
9-2, 138–150	77.84	20.0	3.56	10.8	242	1395	722	12.1	390	<0.1	0.45	9.5
10-3 82–94	88.38	19.6	3.40	10.1	202	1445	733	12.7	350	<0.1	0.30	9.5
11-2, 138–150	97.04	19.9	3.40	10.6	242	1385	681	12.3	375	<0.1	0.20	9.0
12-2, 138–150	106.54	19.9	3.40	10.5	267	1325	673	11.8	375	<0.1	0.20	6.9
14-2, 138–150	125.54	20.1	3.19	10.4	221	1445	681	12.5	320	<0.1	0.20	9.5
15-2, 138–150	135.14	19.8	3.19	10.7	210	1385	711	12.9	375	<0.1	0.20	9.5
17-2, 138–150	154.34	19.3	3.13	10.3	210	1305	688	12.7	400	<0.1	0.20	8.5
18-2, 138–150	163.94	20.3	3.19	10.6	259	1285	696	12.7	360	<0.1	0.20	6.8
20-2, 138–150	184.14	20.2	3.07	10.3	261	1295	711	13.1	330	<0.1	0.20	5.8
Hole 618[h]												
1-2, 140–150	2.95	144.5	1.96	85.0	790	1490	770	15.0	155	2.0	0.60	7.9
2-4, 140–150	12.45	79.3	0.00	46.2	465	1090	242	13.5	125	5.3	0.20	10.8
3-2, 140–150	19.05	66.1	0.00	39.6	400	1180	242	14.5	95	0.5	0.10	14.4
4-2, 140–150	28.65	36.5	0.00	20.0	288	1170	—	16.1	125	0.5	0.10	17.8
5-5, 140–150	42.75	30.4	0.00	16.4	328	1010	301	15.4	155	0.2	<0.05	6.0
6-3, 140–150	49.35	31.7	0.00	17.6	330	1080	342	16.7	190	<0.01	<0.05	5.3
8-1, 140–150	58.35	32.2	0.00	16.9	318	1080	350	17.2	195	<0.1	<0.05	7.3
9-2, 138–150	72.84	35.1	0.00	18.9	360	1245	380	17.7	195	<0.1	<0.05	6.9
10-2, 135–150	77.33	34.4	0.00	17.9	343	1275	305	16.9	195	<0.1	<0.05	8.5
11-1, 135–150	90.53	32.6	0.00	16.9	450	1050	195	13.7	195	<0.1	<0.05	4.0
Hole 618A[i]												
1-1, 5–20	9.33	85.2	0.00	49.7	540	1090	227	13.8	—	0.8	0.10	8.5
1-3, 135–150	13.63	—	0.00	43.0	455	1050	227	13.8	155	0.5	0.10	8.5
2-2, 130–150	31.30	—	0.00	15.7	309	1130	275	15.0	155	0.2	<0.05	11.5
3-3, 124–139	42.32	28.0	0.00	15.4	294	1080	290	15.6	170	<0.1	<0.05	12.0
Hole 619[j]												
1-6, 138–150	9.94	19.4	2.26	10.4	315	1235	380	8.4	260	<0.1	1.60	14.0
3-5, 138–150	17.94	19.4	2.21	10.4	328	1235	390	8.9	235	0.6	0.20	11.5
4-4, 138–150	26.14	19.2	2.09	10.3	300	1190	460	9.5	245	3.3	0.30	11.8
5-3, 138–150	34.34	19.3	1.84	10.2	244	1200	500	10.2	260	3.0	0.30	11.8
6-2, 138–150	42.54	19.7	1.41	10.3	236	1190	475	10.2	160	4.2	0.30	10.4
7-2, 138–150	52.24	13.3	0.96	6.8	140	745	265	7.3	100	7.0	0.15	11.7
8-2, 135–150	61.93	19.5	0.33	10.4	204	1050	385	10.4	155	1.4	0.10	12.0
9-2, 135–150	71.63	19.8	0.00	10.0	194	990	327	12.5	185	1.8	0.10	10.9
10-2, 135–150	75.93	11.7	0.00	6.5	105	590	193	6.5	80	0.7	0.15	8.5
11-2, 135–150	90.93	19.8	0.00	10.2	215	970	279	10.2	115	0.3	0.10	8.0
12-2, 135–150	100.53	15.2	0.00	8.2	181	710	205	7.9	225	0.7	0.25	9.0
13-2, 135–150	110.13	19.8	0.05	10.4	265	930	231	9.5	135	<0.1	0.15	8.4
14-1, 135–150	118.23	19.6	0.16	10.8	265	990	260	10.2	125	<0.1	0.10	10.8
15-2, 135–150	129.32	19.5	0.00	—	290	1080	186	9.6	165	<0.1	0.20	8.3
16-2, 135–150	138.92	17.8	0.00	—	261	940	171	8.6	140	<0.1	0.40	5.7
17-2, 135–150	148.63	19.5	0.00	10.6	296	970	182	8.9	125	<0.1	0.10	4.8
18-2, 112–127	158.10	19.6	0.00	10.4	261	1000	193	9.6	115	<0.1	<0.05	6.1
19-1, 135–150	166.52	20.0	0.20	10.5	248	1030	227	10.3	100	<0.1	<0.05	7.9
20-2, 135–150	177.63	20.4	0.00	—	278	1070	212	9.9	110	<0.1	<0.05	4.0
22-1, 135–150	188.72	20.1	0.00	10.5	294	940	223	9.9	110	<0.1	<0.05	2.4
Hole 619A[k]												
1-3, 135–150	4.43	17.3	2.17	9.6	393	1090	320	7.0	200	0.0	2.30	9.0
Hole 620[l]												
13-2, 135–150	110.73	18.3	3.37	10.0	210	1365	655	11.6	385	6.2	0.15	10.5
14-1, 135–150	118.43	19.2	2.56	10.4	212	1465	744	12.8	430	2.2	0.30	11.3
16-2, 135–150	139.13	19.2	2.76	10.4	225	1435	707	12.5	510	1.6	0.20	11.5
18-5, 135–150	162.82	19.4	3.22	10.3	248	1425	726	11.9	445	0.0	0.20	10.9
21-1, 135–150	185.42	19.0	3.20	10.0	204	1405	707	12.1	345	1.9	0.20	9.5
23-3, 135–150	207.22	19.5	3.20	10.6	227	1375	711	12.2	430	3.9	0.20	10.9
25-5, 135–150	229.22	19.5	3.13	10.6	244	1345	707	12.5	305	3.7	0.30	12.0
28.6, 135–150	259.42	19.2	2.86	10.6	250	1325	655	12.7	265	0.0	0.20	9.5
31-1, 135–150	280.72	19.3	2.81	10.3	231	1305	670	12.1	330	0.0	0.30	8.8
33-3, 135–150	302.92	19.4	2.76	10.5	246	1335	636	12.2	350	<0.1	0.20	9.0
35-2, 135–150	320.63	19.2	2.66	10.2	221	1295	726	12.3	335	0.5	0.40	9.5
40-3, 135–150	369.92	18.9	1.20	9.6	160	1030	473	11.5	140	2.1	0.20	9.0
44-4, 135–150	409.42	11.8	1.33	6.4	140	670	238	6.7	80	2.6	0.15	7.5

Table 1 (continued).

Core-Section (interval in cm)	Sub-bottom depth (m)	Cl (g/kg)	SO$_4$ (g/kg)	Na (g/kg)	K (mg/kg)	Mg (mg/kg)	Ca (mg/kg)	Sr (mg/kg)	Li (μg/kg)	Fe (mg/kg)	Mn (mg/kg)	Si (mg/kg)
Hole 621[m]												
1-2, 138–150	2.94	18.7	1.84	10.6	390	1435	383	8.7	125	<0.1	0.45	10.8
2-5, 138–150	10.94	19.1	0.00	10.6	230	1130	264	11.6	80	<0.1	0.30	13.8
3-5, 138–150	20.54	19.0	0.00	10.0	205	1080	156	11.6	65	<0.1	0.10	11.8
4-4, 140–150	28.65	19.1	0.00	9.8	172	1090	246	13.1	55	<0.1	0.20	12.8
5-3, 128–140	36.64	19.2	0.00	10.0	185	1120	249	13.4	65	<0.1	0.10	12.9
6-2, 138–150	44.84	19.1	0.00	10.0	185	1110	260	13.4	85	<0.1	<0.05	8.8
7-4, 138–150	52.14	19.0	0.30	10.4	185	1140	275	13.4	80	<0.1	0.10	8.5
8-2, 138–150	58.64	19.1	0.00	9.9	160	1160	275	14.4	70	<0.1	0.10	8.8
9-4, 140–150	66.15	19.0	0.00	10.1	156	1200	305	14.4	65	0.7	0.30	13.8
11-1, 138–150	73.34	19.6	0.59	10.3	196	1190	300	14.4	85	<0.1	0.15	6.5
12-3, 0–14	81.87	19.3	0.00	10.1	172	1150	286	14.4	70	<0.1	0.25	9.5
13-1, 128–140	82.74	19.4	0.78	10.4	191	1210	313	14.4	85	<0.1	0.25	7.5
14-2, 135–150	89.63	18.4	0.42	10.1	175	1150	294	14.4	80	0.6	0.25	10.8
15-2, 138–150	97.14	19.3	0.07	10.1	191	1150	264	13.4	80	<0.1	0.15	6.3
16-2, 135–150	102.63	19.1	0.00	10.0	191	2000	238	12.7	70	1.1	0.15	8.0
17-1, 135–150	106.13	19.0	0.04	10.1	191	1080	205	12.8	70	<0.1	0.10	8.8
19-2, 135–150	126.63	19.1	0.00	10.2	238	1010	246	11.3	65	<0.1	0.10	2.4
20-1, 135–150	129.13	19.1	0.06	10.1	196	1070	260	11.6	70	<0.1	0.10	4.0
21-2, 85–100	133.32	19.1	0.00	10.0	175	1070	272	12.1	50	<0.1	0.20	8.5
23-1, 135–150	138.92	19.3	0.00	10.0	183	1090	279	12.2	55	<0.1	0.20	6.8
25-1, 135–150	158.13	19.3	0.00	10.1	276	950	260	11.6	80	<0.1	0.10	1.8
27-1, 135–150	177.32	19.7	0.00	10.8	238	1080	253	12.8	65	<0.1	0.10	8.1
Hole 622[n]												
2-2, 135–150	6.43	19.3	2.34	10.4	322	1200	212	10.0	100	<0.1	0.30	12.3
4-3, 135–150	27.13	19.3	0.00	10.0	191	1180	201	12.5	55	<0.1	<0.05	10.0
6-3, 127–142	46.04	19.3	0.06	10.1	156	1180	257	13.8	65	<0.1	<0.05	10.0
8-2, 135–150	63.73	19.1	0.00	10.5	164	1260	242	13.8	65	<0.1	0.10	16.3
9-2, 135–150	73.73	19.3	0.00	10.1	164	1170	272	14.0	65	<0.1	0.20	14.5
11-3, 135–150	103.32	19.3	0.01	10.0	191	1080	268	10.6	65	<0.1	<0.05	6.0
13-3, 135–150	116.73	19.4	0.00	10.0	187	1100	175	10.9	65	<0.1	<0.05	9.0
15-4, 135–150	129.23	19.3	0.00	10.0	252	1050	182	10.7	110	<0.1	<0.05	6.3
17-1, 135–150	143.92	19.5	0.83	10.2	284	1100	327	13.1	125	0.5	<0.05	12.0
23-1, 135–150	179.13	19.6	1.17	10.3	284	1170	454	13.4	285	<0.1	<0.05	13.8
Hole 623[o]												
1-3, 135–150	4.43	19.3	2.76	10.4	337	1250	469	8.1	270	7.5	0.15	10.8
3-2, 135–150	19.13	18.5	2.96	10.0	202	1395	528	8.9	575	2.3	<0.05	13.3
5-2, 135–150	38.33	19.3	3.05	10.4	210	1425	625	10.3	565	0.6	<0.05	12.9
7-2, 135–150	57.53	18.9	3.00	10.5	200	1490	673	11.9	365	0.8	0.15	10.9
9-5, 0–15	79.88	19.2	2.96	10.4	297	1450	655	11.0	345	6.2	0.15	8.5
11-3, 135–150	97.43	19.1	3.02	10.0	250	1375	636	10.9	545	<0.1	<0.05	9.3
14-2, 135–150	124.32	19.0	2.96	10.4	191	1365	655	11.6	390	2.2	0.10	11.8
17-3, 1–15	152.48	19.4	2.76	10.4	326	1245	580	11.4	320	0.5	0.10	7.8

Note. — means not determined.
[a] 25°04.08′N, 86°08.21′W, water depth 3314 m. Distal end of youngest fan lobe, near channel.
[b] Same as Hole 614.
[c] 25°13.34′N, 85°59.53′W, water depth 3284 m. Distal end of youngest fan lobe, near channel.
[d] Same as Hole 615.
[e] 26°48.67′N, 86°52.83′W, water depth 2999 m. Middle fan eastern margin, 55 km from channel.
[f] Same as Hole 616.
[g] 26°41.93′N, 88°31.67′W, water depth 2478 m. Levee of channel, middle fan.
[h] 27°00.68′N, 91°15.37′W, water depth 2422 m. Orca Basin.
[i] Same as Hole 618.
[j] 27°11.61′N, 91°24.54′W, water depth 2274 m. Pigmy Basin.
[k] Same as Hole 619.
[l] 26°50.12′N, 88°22.25′W, water depth 2612 m. Middle fan overbank deposit.
[m] 26°43.86′N, 88°29.76′W, water depth 2485 m. Channel of middle fan.
[n] 26°41.41′N, 88°28.82′W, water depth 2495 m. Channel, middle fan.
[o] 25°46.09′N, 86°13.84′W, water depth 3188 m. Channel bank, lower fan.

hole. This similarity in behavior of Li and Ca is more clearly shown at other fan sites, although it is never a 1 to 1 correspondence. This similarity is not an analytical artifact resulting from interference by increased Ca, as we proved by spiking samples with additional Ca. These parallel increases in Ca, Mg, Sr, and Li seem likely to have resulted from carbonate dissolution and recrystallization, but could have come from the volcanic ash that

is reported to occur in the sediments (site chapters, this volume). Both carbonate and ash are very minor components of the Leg 96 glacial terrigenous sediment, but even very small amounts of solid can control pore-water composition. Silica concentrations are too erratic to help resolve this question and alkalinity changes are too complex, being a balance between dissolution and precipitation. It seems likely that carbonate precipitation causes

Table 2. Element concentrations in surface seawater samples, DSDP Leg 96.[a]

Site	Cl (g/kg)	Na (g/kg)	Na (%)	K (mg/kg)	K (%)	Mg (g/kg)	Mg (%)	Ca (mg/kg)	Ca (%)	Sr (mg/kg)	Sr (%)	Li (μg/kg)	Li (%)
614	17.41	9.53	98.6	349	100.0	1.13	97.2	383	103.0	6.7	93.2	165	102.0
615	19.99	10.83	97.7	400	100.0	1.27	95.4	428	100.0	8.3	100.0	180	96.8
616	19.88	11.21	101.6	387	97.4	1.29	97.4	432	102.0	8.1	98.7	175	94.7
617	18.43	10.11	98.8	366	99.4	1.18	96.0	398	101.0	7.7	101.1	170	99.3
619	19.33	10.37	96.7	376	97.4	1.25	97.0	420	102.0	8.0	101.4	175	97.4
620	19.76	10.94	99.6	391	99.0	1.30	98.8	432	103.0	8.1	99.3	175	95.3
622	15.72	8.88	101.7	303	96.5	1.02	97.0	331	98.8	6.4	98.6	145	99.2
624	16.15	8.82	98.4	313	97.0	1.06	98.2	353	103.0	7.3	109.4	145	96.6

[a] % is ratio of the value divided by the Cl to the value in the standard seawater divided by the Cl expressed as a %.
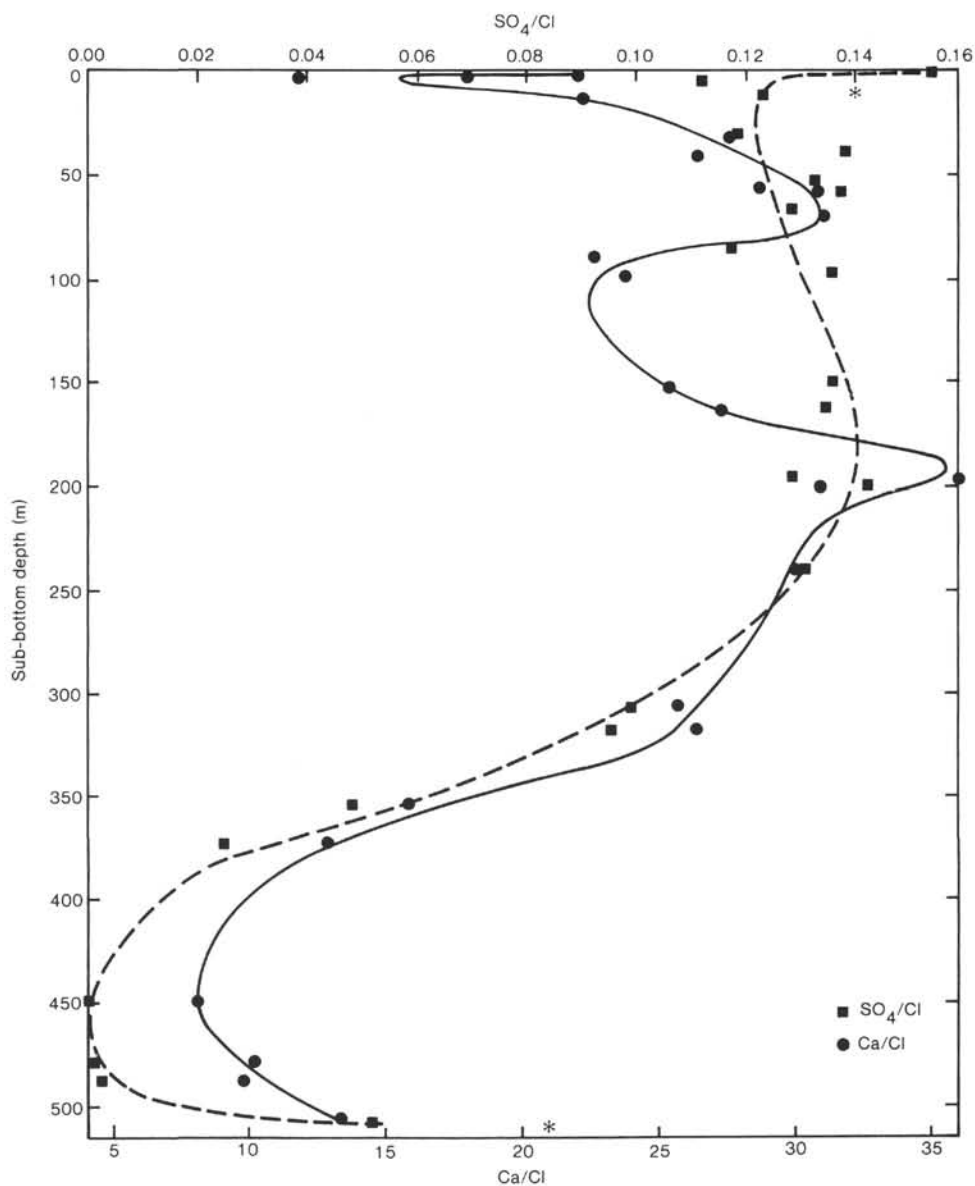
Figure 2. Changes in concentration of Ca and SO_4 with depth in the sediment column at DSDP Site 615. Concentrations are given as ratios to Cl to correct for changes in salinity with depth. The ratios for surface seawater are indicated by an asterisk on the concentration axes.

the decrease in concentration of all these components as bicarbonate and ammonia are produced during sulfate reduction and that carbonate recrystallization causes the increase.

Iron and Mn concentrations are greatly enriched over seawater values at the top of Hole 614 in spite of the lack of sulfate reduction. Apparently oxygen and nitrate have been depleted in these sediments, allowing iron oxides to dissolve. Throughout the Leg 96 samples, dissolved Fe was higher than dissolved Mn, although this is not true in most ocean sediments. High dissolved Fe has been reported in the iron-oxide-rich Gulf of Mexico sediments previously, however (e.g., Trefry, 1977).

Sites 617, 620, 621, and 622 (Middle Mississippi Fan)

The dominant feature of the midfan region is the meandering central channel which, in the vicinity of the Leg 96 drill sites, is about 2 km wide and 40 m deep. It was probably two or three times deeper during periods of active sediment transport and even now is bounded by prominent levees 10–20 m higher than the adjacent seafloor (see Middle Fan Introduction and Summary, this volume). As will be discussed below, we feel that this channel–levee complex created conditions that allowed low-oxygen water to exist in the channel, leading to a contrast in the chemistry of sediments deposited in (Sites 621 and 622) and out (Sites 617, 620) of the channel.

Sites 621 and 622 were located close together in the channel on the outer and inner parts of meander bends, respectively. Each hole penetrated about 200 m of sand and mud which generally became coarser with depth. Pebbles up to 2 cm in diameter were recovered from the bottom of these holes (see site chapters, this volume).

At Site 621, sulfate concentration of the pore water is 35% lower than seawater values at 3 m sub-bottom depth and is undetectable at 11 m (Table 1). At nearby Site 622, sulfate was only 20% lower than seawater values at 6 m but was reduced to 0 above 27 m. The rapid depletion of sulfate at these sites is in stark contrast to the nearby Sites 617 and 620 where sulfate remains at or above seawater concentrations to 200 and 300 m, respectively, and is still at 1/2 the seawater value 400 m sub-bottom at Site 620. The presence of organic debris is mentioned in the shipboard core descriptions and the composition of the sediment is certainly complex and variable both areally and temporally. It is hard to believe, however, that the lithologic character of the sediments was different enough to explain the observed differences in sulfate distribution between the channel and overbank sites. If anything, the overbank sites, being finer grained, would be expected to have more organic matter and more reducing capacity, exactly the opposite of our observations.

One explanation of the "sulfate paradox" on the middle fan is that the channel acted to restrict bottom-water circulation leading to low oxygen concentrations in the bottom water in the channel and hence less oxidation of labile organic matter at the sediment/water interface. Burial of this labile organic matter by the rapidly depositing sediment would lead to rapid sulfate reduction. Sedimentation rates alone cannot be a factor as they are approximately the same inside and outside of the channel (Wetzel and Kohl, this volume; site chapters, this volume). Present-day redox potential in the sediment column may also be relatively unimportant as it seems to be low in both channel and overbank deposits, allowing Fe to dissolve. If the channel was as deep as 200 m in the past, as has been suggested in the introductory chapter (this volume), and only a kilometer or so wide, circulation within the channel could certainly have been restricted. We have no data on oxygen levels in the bottom water in the channel at the present time, although this may give a clue to past conditions.

As is always the case, other changes accompany sulfate reduction at Sites 621 and 622. Calcium, for example, drops to 1/2 or less that of the overlying seawater value at the point where sulfate goes to 0, because of bicarbonate production as discussed earlier. Interestingly, calcium concentrations increase where sulfate is found at depth in the sediment column, as it is at several isolated depths at Site 621 and very clearly at depth at Site 622. These are apparently relict values produced during times of high oxygen in the channel bottom water and not enough time has elapsed to allow them to diffuse completely away.

Magnesium shows a weak tendency to follow the Ca depletions at Sites 621 and 622, but the trends are interrupted by isolated high values. Strontium is about 50% higher than seawater levels throughout both holes as it is in the overbank deposits at Sites 617 and 620. In fact, strontium remains in a rather narrow range for all Leg 96 samples. The two high values found in the carbonate ooze at the bottom of Hole 615 are exceptions already discussed and there are a few other samples enriched by 75–100% over seawater values rather than the ubiquitous 50–60% enrichment found for most samples. Although strontium shows almost no tendency to decrease when calcium carbonate is precipitated at these sites, it increases with calcium carbonate dissolution. The Ca trend for Site 622 is shown in Fig. 3.

Lithium is a very minor component in the pore water, but has shown consistent trends at many sites on previous DSDP legs (Presley and Kaplan, 1970; Gieskes, 1983), most often related to the volcanic component in the sediments. The trends at Sites 617, 620, 621, and 622 are pronounced, but are probably not related to volcanism. Rather they seem related to changes in Ca, presumably carbonate dissolution and precipitation. The contrast between channel and overbank deposits is marked. In the channel, where sulfate reduction causes carbonate to precipitate, lithium concentrations decrease to 1/3 of the seawater value. In contrast, in the overbank deposits, both calcium and lithium increase almost twofold. The Ca and Li profiles are not identical but are certainly similar (Figs. 3, 4).

Potassium, which is more prone to sampling artifacts than the other major ions, shows a rapid depletion with depth at all midfan sites to values near 1/2 that of normal seawater. This pattern is typical of all sites sampled on Leg 96 but, as with other constituents, trends are often interrupted by isolated high values at various depths probably because of the interbedded nature of the sand,
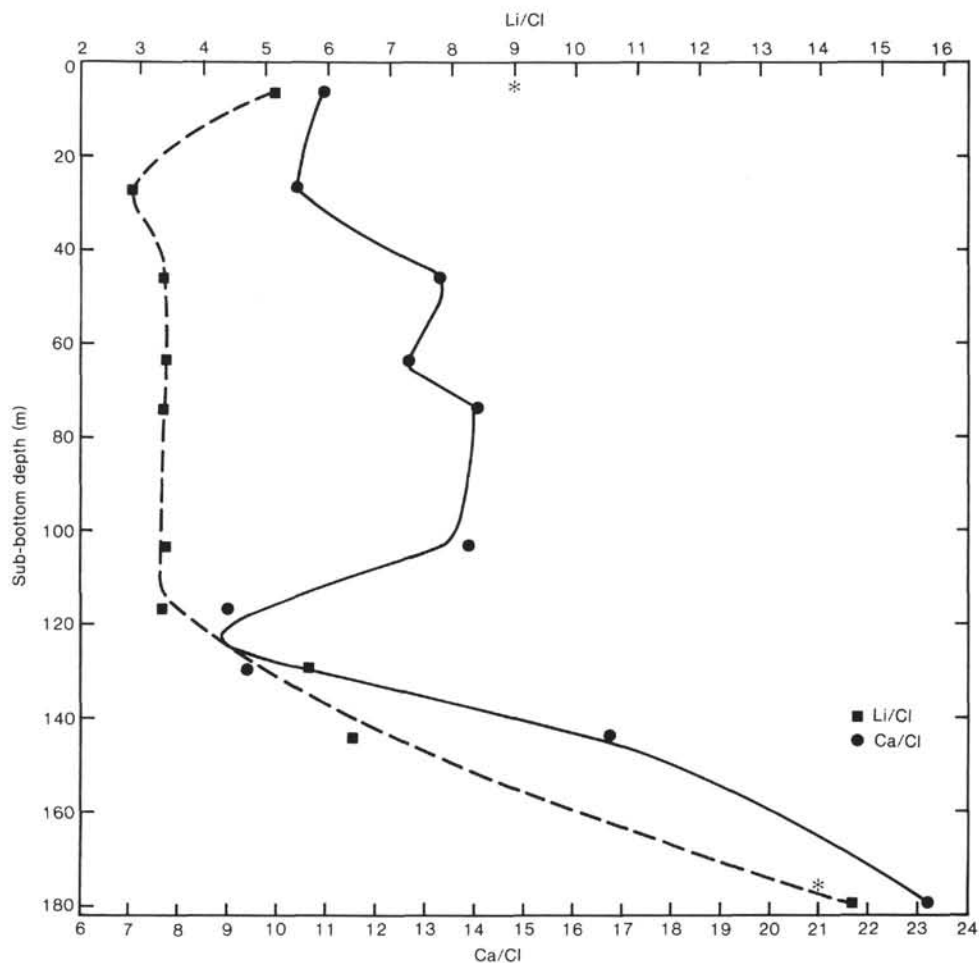
Figure 3. Changes in concentration of Ca and Li with depth in the sediment column at DSDP Site 622. Concentrations are given as ratios to Cl to correct for changes in salinity with depth. The ratios for surface seawater are indicated by an asterisk on the concentration axes.

silt, and mud recovered on Leg 96. This varying lithology should have an effect on all inorganic geochemistry trends, but we have not been able to correlate observed chemical changes with lithologic changes shown on the shipboard logs. Uptake of K, as is observed, would be expected if montmorillonite clays are converted to illite, but this is usually thought to occur deeper in the sediment column (at higher temperatures) than the intervals sampled here (e.g., Perry and Hower, 1970).

Site 616 (Mississippi Fan Margin)

Site 616 was drilled 55 km northeast of the central channel on the fan margin in what has been described as a massive slump deposit which covers the youngest fan lobe with about 100 m of mass-transported material. It is estimated that almost 40% of the sediment in the 88-m-thick upper fan lobe is sand; the underlying fan lobe is much muddier, containing only 7% sand. The slump deposit that overlies these fan lobe sediments consists of steeply dipping interbedded mud and silt beds (Site 616 chapter, this volume).

The pore water at Site 616 resembles that in the overbank deposits at Sites 617 and 620 and differs from that of the channel deposits at Sites 621 and 622 (Table 1).

For example, sulfate concentration remains high to depths of 300 m and decreases by only about 25% from there to the bottom of the hole. Sulfate is, in fact, enriched relative to seawater of equivalent chlorinity by 20 to 30% throughout the upper 150 m at Site 616. The same phenomenon occurs at Site 617, where sulfate enrichments extend to the bottom of the hole, at Site 620 where enrichments can be found to 230 m, and at Site 623 with enrichment to 125 m sub-bottom. It appears that all pore water of late Wisconsin glacial age is enriched in sulfate except that which has undergone subsequent sulfate reduction. There is no obvious explanation for this phenomenon. The SO_4 data reported here are reliable because Ishizuka, Kawahata, et al. (this volume) report values similar to ours using a different technique and we obtained similar values for selected samples by a third independent method (precipitation and weighing of $BaSO_4$). We have not seen this phenomenon elsewhere, but it is probably related to Pleistocene sea-level changes.

Exposure of the northern Gulf of Mexico continental shelf by lower sea level and the resulting rapid seaward transport of sediment could have moved gypsum from salt dome cap rocks as a detrital mineral. Dissolution of gypsum would add Ca and sulfate to the pore water in a
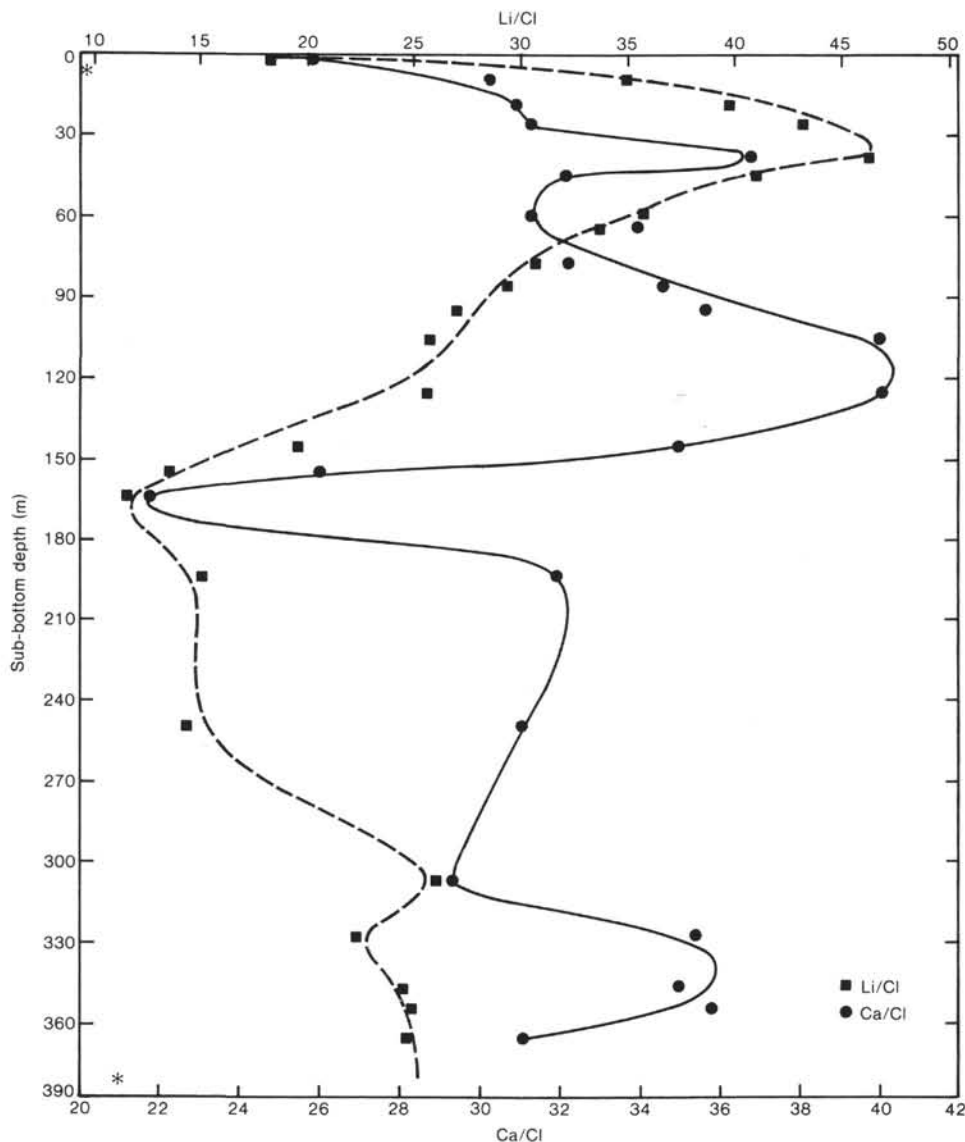
Figure 4. Changes in concentration of Ca and Li with depth in the sediment column at DSDP Site 616. Concentrations are given as ratios to Cl to correct for changes in salinity with depth. The ratios for surface seawater are indicated by an asterisk on the concentration axes.

1 to 1 molar ratio, which is about what is seen in many Leg 96 samples, although the correspondence is far from perfect. However, both Ca and SO_4 would likely have undergone subsequent reactions (sulfate reduction, carbonate precipitation, etc.) making preservation of the original ratios unlikely. If the Ca enrichment seen in these samples is from carbonate dissolution or leaching of volcanic ash, rather than from gypsum dissolution, then the sulfate is most likely to have been added from oxidizing pyrite. This would result from lowered sea level and erosion of reducing sediments from the shelf. Pyrite, as suggested for gypsum, would also become a detrital mineral and be oxidized to release SO_4 after deposition. This second explanation is strongly supported by S isotope data we have obtained on selected samples of dissolved sulfate. The values show strong depletion in the heavy S isotopes, as occurs in pyrite. It is surprising that this mechanism produces the observed widespread

and generally uniform SO_4 enrichments found on the Mississippi Fan, but we have no other explanation at this time.

As mentioned above, Ca is enriched in all Site 616 pore waters (Fig. 4). Relative to Cl, the enrichments reach a maximum at 100 m sub-bottom and then gradually and erratically decrease below that depth, in concert with sulfate behavior. Lithium also follows this behavior, showing an enrichment everywhere with a maximum at 40 m, where there is a local Ca maximum, and a decrease with depth to a minimum at 175 m, coincident with the Ca minimum (Fig. 4). Potassium values are relatively constant but low throughout the hole.

Sites 618 and 619 (Continental Slope Basins)

The continental slope off Louisiana and eastern Texas is very irregular, with numerous topographic highs and intervening lows (Bouma, 1983). The highs are the

expression of underlying salt diapirs, which in a few places reach or come close to the sediment/water interface. The depressions between the highs, the intraslope basins, are of various sizes and shapes. Two of these were sampled on Leg 96, Pigmy Basin and Orca Basin (see Sites 618 and 619 chapters, this volume). Sedimentation in these basins has been much more rapid than that on the Mississippi Fan during Holocene times, but during the Pleistocene the opposite was true.

Pigmy Basin is of the blocked-canyon type described by Bouma (1983) as formed by a salt diapir that blocked off a submarine canyon trapping sediment behind it. This situation should result in coarse material being trapped during low stands of sea level with more clay-rich material with rising sea level. Sediments recovered from Hole 619 are dark gray clays with sand and silt laminae occurring throughout but increasing in abundance toward the base of the hole, especially below 150 m sub-bottom (see Site 619 chapter, this volume). Calcium carbonate con-

tent also varies erratically throughout the hole and two thin volcanic ash beds were found at 141-m depth. Sedimentation rates were about 42 cm/1000 yr. in the Holocene (top 10 m), 195 cm/1000 yr. for the late Wisconsin glacial (136 m thick) and 24 cm/1000 yr. for the Wisconsin interstadial (10 m thick) (Site 619 chapter, this volume). The hole may have bottomed in early Wisconsin glacial deposits (Kohl, this volume).

Pore waters from the Pigmy Basin sediments show a fairly predictable composition based on the nature of the sediments, which were dark, black in places, and contained small amounts of biogenic gas. Sulfate reduction was to be expected in these sediments and was found, even in the shallowest sample recovered (4.4 m sub-bottom, Table 1). Sulfate concentration decreases downhole rather smoothly, from a surface value that is 20% lower than the normal seawater value to 0 at about 70-m depth (Fig. 5). This sulfate decrease was accompanied by a Ca decrease, but only after Ca concentration had gone
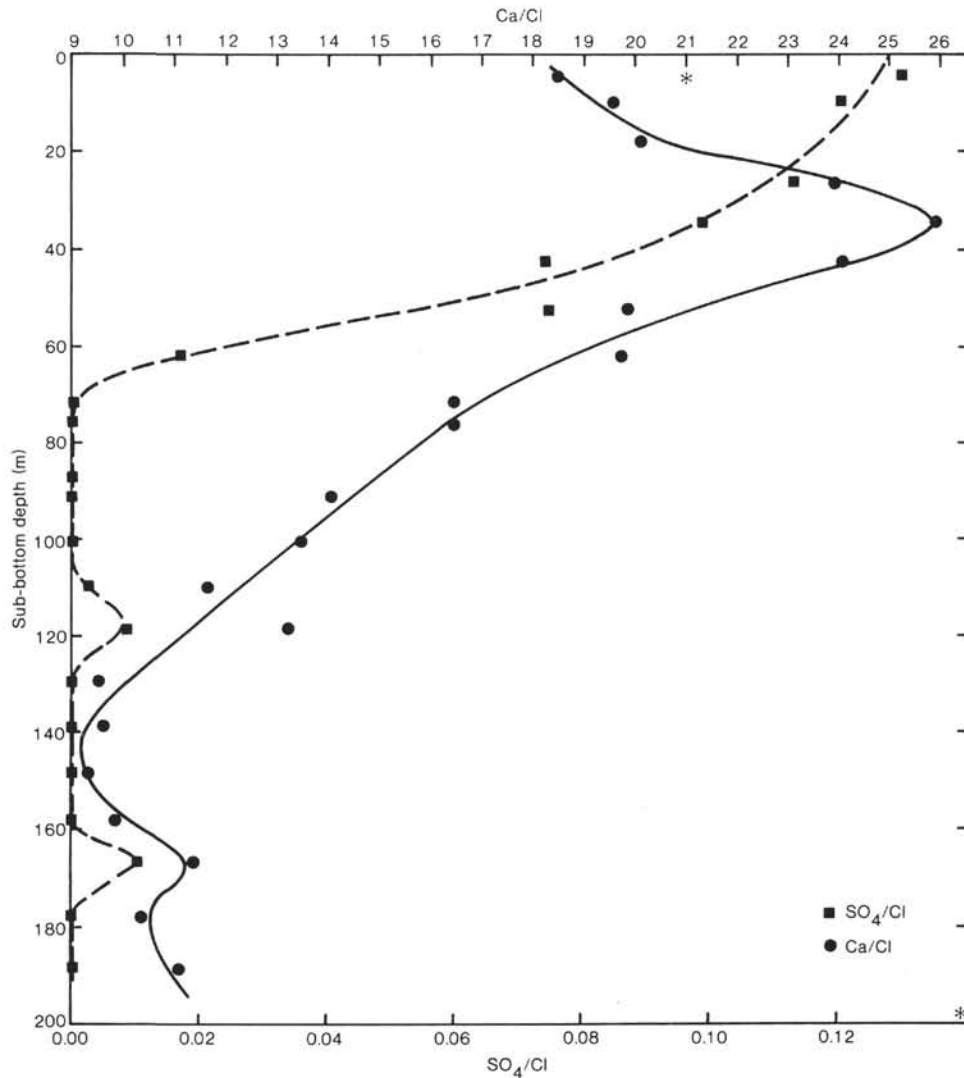

Figure 5. Changes in concentration of SO_4 and Ca with depth in the sediment column at DSDP Site 619. Concentrations are given as ratios to Cl to correct for changes in salinity with depth. The ratios for surface seawater are indicated by an asterisk on the concentration axes.

through a local maximum at 35-m depth where it was 20% higher than average seawater (Fig. 5). These enriched Ca values may be residue of even higher values from glacial times, as discussed above for Site 616, but the increase from 18 to 34 m would not be explained by this mechanism. Active sulfate reduction is occurring, which lowers the Ca concentration, but some unknown competing process is causing the Ca increase in the top 40 m of the sediment column.

Lithium, as in all Leg 96 samples, follows Ca trends rather closely, with 30–40% enrichment at the top of the hole and an abrupt decrease to values lower than seawater that accompanies the Ca decrease below 40 m. Depletion in lithium is about 40% below 150-m depth. Strontium trends parallel Ca to some extent, but are generally more erratic and lower in concentration than samples from the Mississippi Fan. Potassium values follow the Ca decrease in the top 75 m, but then increase to a well-defined broad maximum between 120 and 140 m (Fig.

6). This increase in potassium may be related to the volcanic ash beds found at 141-m depth (site chapter, this volume). Mg shows a similar decrease to about 100 m and an increase from 100 to 150 m sub-bottom (Fig. 6). Silicon decreases rather monotonically through the hole and gives no indication of dissolving volcanic ash.

According to the Bouma (1983) classification, Orca Basin is an interdomal type basin that formed by coalescing salt diapirs completely enclosing a depression. Cut off from bottom-transported material, it should therefore be filled with fine-grained hemipelagic and pelagic sediment. Orca Basin is unique in that it contains an anoxic brine pool in its bottom 200 m (Shokes et al., 1977). The brine precludes all organic activity in the basin other than bacterial, which leads to highly reducing, intricately laminated sediment (Trabant and Presley, 1978; Sheu and Presley, in press).

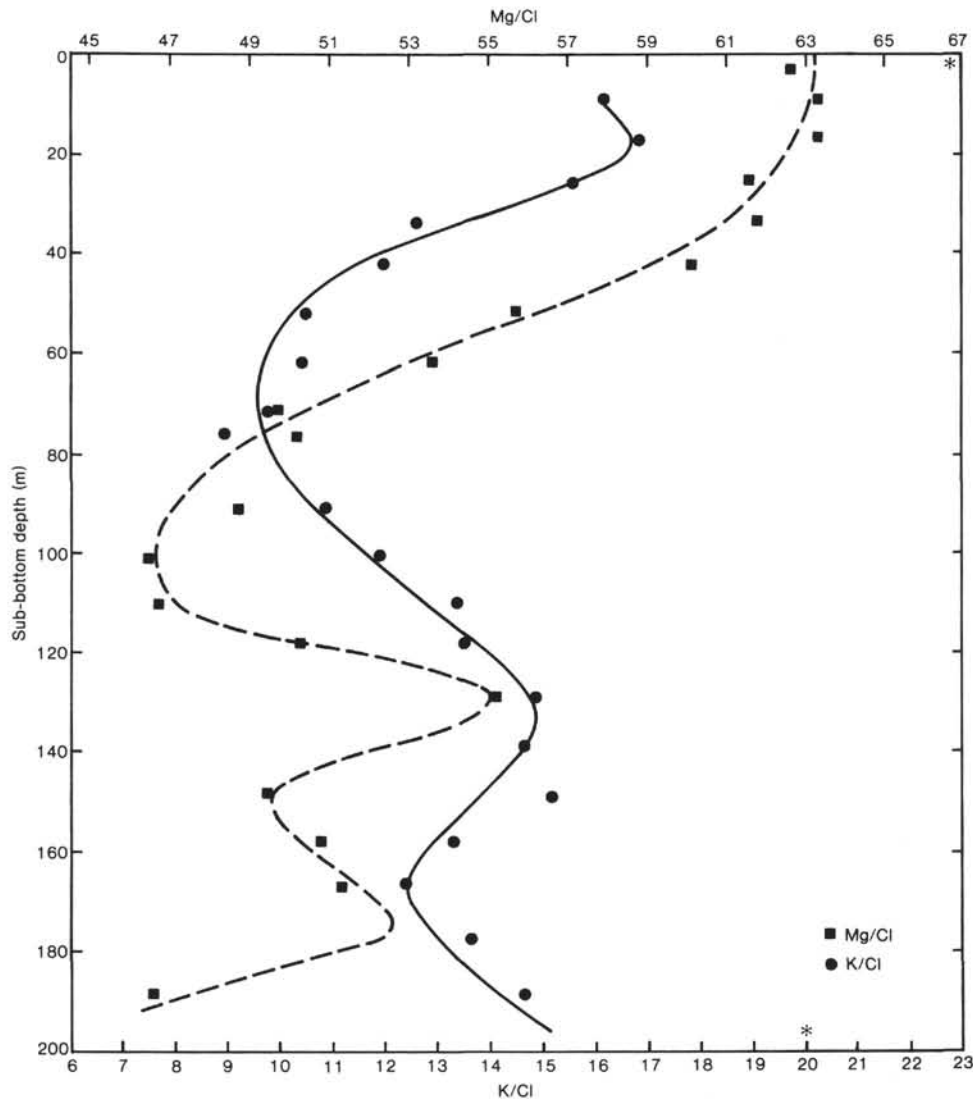The Orca Basin brine is basically seawater that has been enriched with NaCl to near saturation. The source

Figure 6. Changes in concentration of K and Mg with depth in the sediment column at DSDP Site 619. Concentrations are given as ratios to Cl to correct for changes in salinity with depth. The ratios for surface seawater are indicated by an asterisk on the concentration axes.

of the salt is almost certainly a nearby salt dome exposed on the seafloor; the brine is also enriched somewhat in Ca and SO_4 from the salt dome caprock (Shokes et al., 1977). Relative to Na or Cl, however, Ca, SO_4, and all other constituents are greatly depleted in the Orca Basin brine and in the interstitial water. The concentrations of Ca, Mg, K, and Li normalized to Cl versus depth for the Site 618 samples show straight line increases to about 40-m depth where salinity becomes constant. Below that depth, K, Mg, and Li are nearly constant, whereas Ca, which is already depleted, shows a further decrease toward the bottom of the hole. Strontium is relatively constant with depth at about twice the seawater values, and is independent of salinity variations. In fact, this salinity independence applies to everything except Na and Cl, and thus increased salinity caused by dissolving NaCl does not seem to have affected reactions between the dissolved ions and clay or carbonate in the sediment. Site 618 data support our previous interpretations that the high salinity does not affect the rate of sulfate reduction (Sheu and Presley, 1982); even Li is independent of the added Na.

It has been known from the earliest sampling in the Orca Basin that the salinity of the pore water decreases with depth (Shokes et al., 1977). Therefore, the source of the high salinity brine pool in the basin is not from upward diffusion of salt buried immediately below the basin. Rather, the source of brine must be from exposed salt diapirs somewhere on the surrounding basin walls, from which it has flowed down to partially fill the basin. This source cannot, however, be far from the present brine/seawater interface or mixing with seawater during downslope transport of the brine would lower its salinity below its present near saturation with NaCl.

The salinity gradient observed in the Site 618 sediment pore water looks like one established by downward diffusion. If this is the case, it is possible to calculate the time needed for its establishment. This calculation is not simple for it must consider sediment accumulation during diffusion and porosity variations which affect diffusion. Addy and Behrens (1980) considered these factors in calculating the time needed to establish the salinity gradient they observed in an 11-m piston core from the basin. They concluded that brine had first entered the basin and set up anoxic conditions about 8000 yr. ago.

The Leg 96 shipboard party interprets the upper 11 m of sediment recovered at Site 618 as a slump deposit overlying Holocene sediment. Despite this, the salinity gradient observed in the pore water decreases through the upper 11 m smoothly and continues to 30-m depth, although relatively few points are available to define the gradient. The gradient is similar to the one found by Addy and Behrens (1980) and would take at least as long to establish (8,000–10,000 yr.) It seems unlikely, then, that the upper 11 m of sediment has been emplaced by slumping during the Holocene.

Drilling at Site 618 allowed the salinity gradient to be traced much deeper than had been possible before, with the rather surprising result that salinity becomes relatively constant at about 50‰ below 30-m depth. This observation proves that stagnation, and therefore anoxic conditions, were established in the Orca Basin much earlier than 8000 yr. ago. The minimum sedimentation rate determined by the shipboard scientists (Wetzel and Kohl, this volume) dates the bottom of the hole at about 85,000 yr. ago, a number certainly too large. If the sedimentation rate is twice as high as the estimated minimum, and therefore similar to the rate in the nearby Pigmy Basin, the bottom sample would be about 50,000 yr. old. As there was no clear indication of a salinity decrease in the bottom 60 m of the hole, it seems that the 50,000 yr. is a minimum time for the existence of high salinity, stagnation, and anoxia in Orca Basin.

CONCLUSIONS

The Leg 96 samples were collected 300–600 km from shore and in water depths of 2500–3000 m, yet they had accumulated extremely rapidly and texturally and lithologically were near-shore deposits. Interstitial water chemistry at some sites showed typical near-shore behavior, with rapid sulfate reduction, calcium depletion, alkalinity increases and other evidences of bacterially mediated diagenesis. At other sites these reactions became evident only at a sediment depth of 100 m or more, behavior typical of deep-sea sediments. Variations in grain size, mineralogy, total organic carbon, and sedimentation rate (reported elsewhere in this volume) cannot explain these differences in rates of diagenetic reactions. They are, instead, apparently caused by differences in bottom-water oxygen levels at the time of deposition. When bottom water circulation is restricted, for example in a deep channel or a basin, oxygen levels decrease and labile organic matter is buried rather than being oxidized at the sediment/water interface. This results in rapid sulfate reduction and other diagenetic reactions as seen at Sites 618, 619, 621, and 622.

Calcium and sulfate concentrations in many of the Leg 96 interstitial waters were higher than normal seawater values. Enrichments in calcium have been noted in many previous DSDP samples (e.g., Gieskes, 1983) but sulfate enrichment is very unusual, not only for DSDP samples but for any interstitial water (e.g., Manheim, 1976; Presley and Trefry, 1980; Gieskes, 1983). Furthermore, in Leg 96 samples calcium enrichments occur at shallow depths and accompany sulfate enrichments, whereas on previous legs calcium enrichments were only seen at a depth in the sediment column where sulfate was at or below seawater values. Dissolving gypsum would produce the calcium and sulfate enrichments seen in the Leg 96 samples, but so would oxidation of pyrite which would release both sulfate and acid to dissolve calcium carbonate. Preliminary sulfur isotope data (not reported here) supports the pyrite oxidation hypothesis. Rapid erosion and redeposition of reducing shelf sediment during Pleistocene sea-level lowering would provide a source of detrital pyrite to the sediment, pyrite which would then be oxidized by oxygen, nitrate, iron oxide, and other oxidizing agents. Calcium carbonate dissolution in Gulf of Mexico sediments which has been attributed in the past

to organic matter oxidation and production of CO_2 (Huang and Goodell, 1970; Joyce, 1984) may rather be the result of detrital pyrite oxidation.

Site 618 in the Orca Basin was drilled through a hypersaline brine pool. Based on the samples available, the interstitial water salinity seems to decrease smoothly with depth and gives no indication of slumping or sediment mass movement. The interstitial water salinity at the bottom of the hole (90 m sub-bottom) is about 50‰, thus high salinity and resulting stagnation have existed in the Orca Basin for much longer than previously thought (Addy and Behrens, 1980).

Interstitial water analysis has revealed features of the environment of deposition and diagenesis of Leg 96 sediment which could not have been deduced in any other way.

REFERENCES

Addy, S. K., and Behrens, W. E., 1980. Time of accumulation of hypersaline anoxic brine in Orca Basin (Gulf of Mexico). *Mar. Geol.*, 37:241–252.

Bouma, A. H., 1983. Intraslope basins in the northwest Gulf of Mexico: a key to ancient submarine canyons and fans. *Am. Assoc. Pet. Geol. Spec. Publ.*, 32:567–581.

Ericson, D. B., and Wollin, G., 1968. Pleistocene climates and chronology in deep-sea sediments. *Science*, 162:1227–1234.

Gieskes, J. M., 1983. The chemistry of interstitial water of deep-sea sediments: Interpretation of deep sea drilling data. *In* Riley, J. P., and Chester, R. (Eds.), *Chemical Oceanography* (Vol. 8): London (Academic Press).

Huang, T. C., and Goodell, H. G., 1970. Sediments and sedimentary processes of the eastern Mississippi cone, Gulf of Mexico. *Am. Assoc. Pet. Geol. Bull.*, 54:2070–2100.

Joyce, J. E., 1984. Preservation of aragonite in late Pleistocene sediments in the deep basin of the western Gulf of Mexico [Ph.D. dissert.]. Texas A&M University, College Station.

Manheim, F. T., 1976. Interstitial waters of marine sediments. *In* Riley, J. P., and Chester, R. (Eds.), *Chemical Oceanography*; New York (Academic Press), pp. 115–181.

Manheim, F. T., and Sayles, F. L., 1974. Composition and origin of interstitial water of marine sediments, based on deep-sea drill cores. *In* Goldberg, E. D. (Ed.), *The Sea* (Vol. 5): New York (Wiley).

Manheim, F. T., and Waterman, L. S., 1974. Diffusimetry (diffusion constant estimation) on sediment cores by resistivity probe. *In* von der Borch, C. C., Sclater, J. G., et al., *Init. Repts. DSDP*, 22: Washington (U.S. Govt. Printing Office), 663–670.

Perry, E. A., Jr., and Hower, J., 1970. Burial diagenesis in Gulf Coast pelitic sediments. *Clays Clay Miner.*, 18:165–177.

Presley, B. J., 1971. Techniques for analyzing interstitial water samples. Part I. Determination of selected minor and major constituents *In* Winterer, E. L., Riedel, W. R., et al., *Init. Repts. DSDP*, 7, Pt. 2: Washington (U.S. Govt. Printing Office), 883–887.

Presley, B. J., and Kaplan, I. R., 1970. Interstitial water chemistry: Deep Sea Drilling Project, Leg 4. *In* Bader, R. G., Gerard, R. D., et al., *Init. Repts. DSDP*, 4: Washington (U.S. Govt. Printing Office), 415–430.

Presley, B. J., and Trefry, J. H., 1980. Sediment–water interactions and the geochemistry of interstitial water. *In* Olausson, E., and Cato, I. (Eds.), *Chemistry and Biochemistry of Estuaries*: New York (Wiley), pp. 187–232.

Sheu, D. D., and Presley, B. J., 1982. Sulfate reduction in Orca Basin sediments. *Abstr. Annu. Mtgs. Am. Geophys. Union, Winter 1982, San Antonio.*

_____, in press. Variations of calcium carbonate, organic carbon and iron sulfides in anoxic sediment from Orca Basin, Gulf of Mexico. *Mar. Geol.*

Shokes, R. F., Trabant, P. K., Presley, B. J., and Reid, D. F., 1977. Anoxic hypersaline basin in the Northern Gulf of Mexico. *Science*, 196:1443–1446.

Strickland, J. D., and Parsons, T. R., 1968. A practical handbook of seawater analysis. *Fish. Res. Board Canada Bull.*, 167:1–311.

Trabant, P. K., and Presley, B. J., 1978. Orca Basin, anoxic depression on the continental slope, northwest Gulf of Mexico. *In* Bouma, A. H., Moore, G. T., and Coleman, J. M. (Eds.), *Am. Assoc. Pet. Geol. Stud. Geol.* (Vol. 7):Tulsa (Am. Assoc. Pet. Geol.), 303–311.

Trefry, J. H., 1977. The transport of heavy metals by the Mississippi River and their fate in the Gulf of Mexico. [Ph.D. dissert.]. Texas A&M University, College Station.